INVESTIGATION ON THE CORROSION BEHAVIOR OF HAHA-4 CLADDING BY OXIDE CHARACTERIZATION

JEONG-YONG PARK*, BYUNG-KWON CHOI and YONG HWAN JEONG
Fusion Technology Division, Korea Atomic Energy Research Institute
1045 Daedeokdaero, Yuseong-gu, Daejeon 305-353, Korea
*Corresponding author. E-mail : parkjy@kaeri.re.kr

Received December 20, 2008
Accepted for Publication January 10, 2009

The microstructure, the corrosion behavior and the oxide properties were examined for Zr-1.5Nb-0.4Sn-0.2Fe-0.1Cr (HANA-4) alloys which were subjected to two different final annealing temperatures: 470°C and 570°C. HANA-4 was shown to have ß-enriched phase with a bcc crystal structure and $Zr(Nb,Fe,Cr)_2$ with a hcp crystal structure with ß-enriched phase being more frequently observed compared with $Zr(Nb,Fe,Cr)_2$. The corrosion rate of HANA-4 was increased with an increase of the final annealing temperature in the PWR-simulating loop, 360°C pure water and 400°C steam conditions, which was correlated well with a reduction in the size of the columnar grains in the oxide/metal interface region. The oxide growth rate of HANA-4 was considerably affected by the alloy microstructure determined by the final annealing temperature.

KEYWORDS : Fuel Claddings, Zr Alloys, Corrosion, Oxide, Microstructure

1. INTRODUCTION

Advanced Zr fuel claddings have been developed continuously with a focus on an improvement of the corrosion resistance[1-3] since waterside corrosion of fuel claddings is one of the main limitations to burn-up extension of nuclear fuels. Recently, a series of Nb-containing Zr alloys named HANA has been developed to improve the corrosion resistance of fuel claddings on the basis of the correlations between the corrosion behavior and the metallurgical factors including the chemical composition, the microstructure and the precipitate characteristics[1].

HANA alloys exhibited excellent corrosion resistance in the out-reactor as well as the in-reactor conditions when compared to Zircaloy-4[1]. It was revealed that the corrosion rate of HANA alloys increased with an increase of the final annealing temperature irrespective of the alloy composition[4]. However, its mechanism has not yet been clarified partly due to the lack of an oxide characterization.

This investigation aims at understanding the effect of a final annealing temperature on the corrosion and the oxide properties of Nb-containing Zr alloys. In this study, the microstructure, the corrosion behavior and the oxide properties were examined for Zr-1.5Nb-0.4Sn-0.2Fe-0.1Cr alloy which was subjected to different final annealing conditions.

2. EXPERIMENTAL PROCEDURE

The alloy used in this study was the HANA-4 with a nominal composition of Zr-1.5wt%Nb-0.4wt%Sn-0.2wt%Fe-0.1wt%Cr. The analyzed chemical composition of HANA-4 is shown in Table 1. HANA-4 alloys were fabricated as cladding tubes with an outer diameter of 9.5 mm and a wall thickness of 0.57 mm. The manufacturing process of the HANA-4 tubes consisted of vacuum arc remelting, hot forging, ß-quenching, extrusion and four pilgerings followed by an annealing. The intermediate annealing was performed at 570 to 580°C for 2 to 3 h. The final annealing was performed at 470°C and 570°C to investigate its effect on the corrosion behavior of HANA-4 alloy.

The microstructure of the HANA-4 alloy was observed using transmission electron microscopy (TEM). The samples for TEM observation were prepared by thinning a tube to a thickness of less than 70 μm in a solution of 10 vol.% HF, 30 vol.% H_2SO_4, 30 vol.% HNO_3 and 30

Table 1. Analyzed Chemical Composition of HANA-4 (wt%)

Nb	Sn	Fe	Cr	Zr
1.45	0.41	0.22	0.10	Bal.

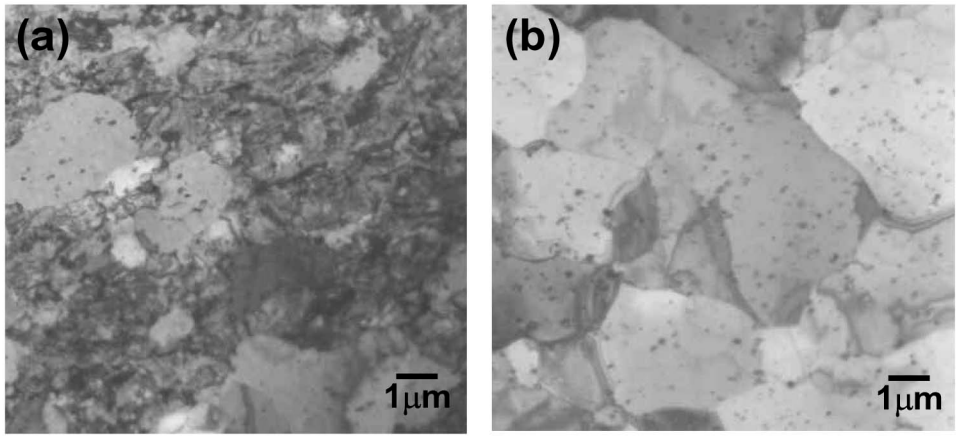

Fig. 1. Transmission Electron Micrographs of HANA-4 Alloys which were Final-Annealed at (a) 470°C and (b) 570°C

vol.% H_2O followed by a twin jet polishing with a solution of 10 vol.% $HClO_3$ and 90 vol.% C_2H_5OH. The precipitates in the HANA-4 alloys were identified by analyzing a selected area diffraction pattern (SADP) and the chemical composition obtained from an energy dispersive X-ray spectroscopy (EDS).

The corrosion test specimens were cut into segment tubes with a length of 40 mm and then pickled in a solution of 10 vol.% HF, 30 vol.% H_2SO_4, 30 vol.% HNO_3 and 30 vol.% H_2O. The corrosion test was performed in three different corrosion environments: a PWR-simulating loop, 360°C pure water and 400°C steam. The PWR-simulating loop was operated at a temperature of 360°C, a pressure of 18.5 to 18.8 MPa, a flow rate of 3 to 4 liter/h and a pH of 6.8. The concentration of Li and B in the water was controlled at 2.2 wppm and 650 wppm, respectively and the dissolved oxygen content was maintained at less than 5 wppb during a 1000 days operation of the PWR-simulating loop. The corrosion behavior of the alloys was evaluated by measuring the weight gain of the corrosion test specimens which were periodically taken out of the loop.

The oxide microstructure was observed by a TEM for the cross section of the corroded specimens in the PWR-simulating loop condition. The corroded specimens were sliced to a thickness of 300 μm and then mechanically polished to less than 20 μm. The mechanically thinned samples were ion-milled by a focused ion beam using NOVA 600.

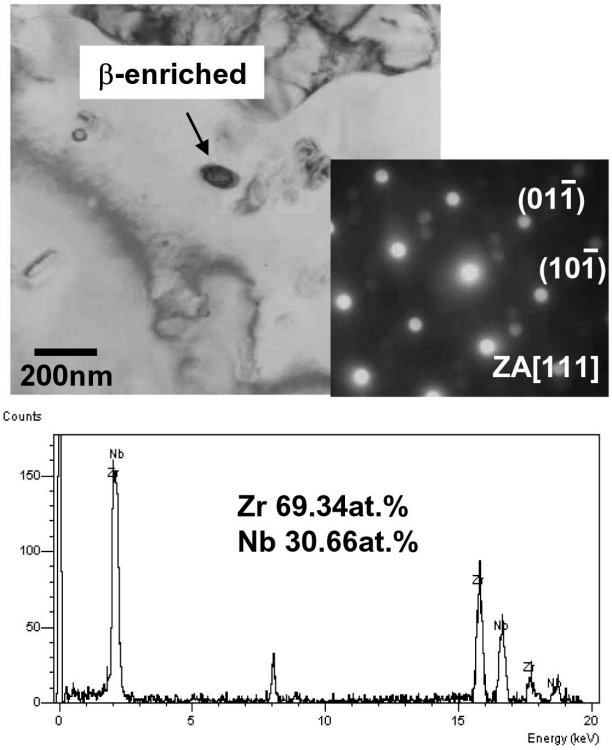

Fig. 2. ß-Enriched Precipitate Observed in HANA-4 Alloy which was Final-Annealed at 470°C

3. RESULTS AND DISCUSSION

3.1 Microstructure

Fig. 1 shows the microstructure of the HANA-4 annealed at 470°C and 570°C. The microstructure of the HANA-4 annealed at 470°C consisted of entangled dislocations and recrystallized grains with a number of precipitates. When the final annealing temperature was increased from 470°C to 570°C, the entangled dislocations disappeared and the size of the recrystallized grain was increased.

The precipitates in HANA-4 were identified by analyzing the SADP and the chemical compositions obtained form the EDS. The analysis on the precipitates revealed that the HANA-4 had two types of precipitates.

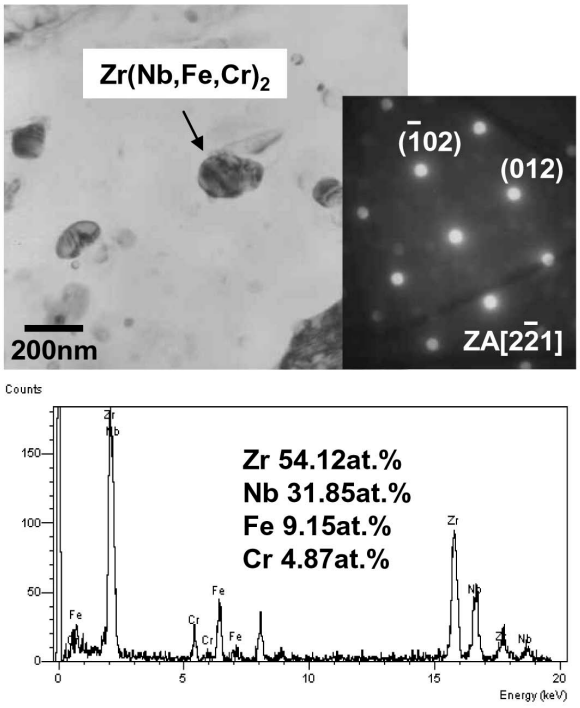

Fig. 3. $Zr(Nb,Fe,Cr)_2$ Precipitate Observed in HANA-4 Alloy which was Final-Annealed at 470°C

Figs. 2 and 3 show ß-enriched phase with a bcc crystal structure and $Zr(Nb,Fe,Cr)_2$ with a hcp crystal structure found in the HANA-4 annealed at 470°C. Table 2 summarizes the characteristics of the precipitates in the HANA-4. ß-enriched phase were more frequently observed when compared to $Zr(Nb,Fe,Cr)_2$ precipitates in HANA-4 alloy irrespective of the final annealing temperature.

Although the precipitate types of HANA-4 were not changed as the annealing temperature increased from 470°C to 570°C, the average particle size of the precipitates increased from 70 nm to 90 nm as shown in Table 2. The intermediate annealing temperature during the manufacturing process was the same before a final annealing. Therefore, the final annealing temperature at 470°C is likely to be responsible for a finer precipitate size even though the precipitate size is affectd more by the intermediate annealing temperature.

3.2 Corrosion Properties

Fig. 4 shows the corrosion behavior of HANA-4 with two different final annealing conditions in various corrosion environments including a PWR-simulating loop, 360°C pure water and 400°C steam conditions. The corrosion rate was highest in 400°C steam and lowest in the PWR simulating loop condition for a given annealing temperature. The corrosion rate in the 360°C water condition was slightly higher than that in the PWR-simulating condition even though the corrosion temperature was 360°C in both corrosion environments. One possible cause is the fact that the dissolved oxygen concentration was controlled to be much lower in the PWR simulating loop condition.

The corrosion rate was increased with an increase of the final annealing temperature regardless of the corrosion environment. This implies that the corrosion rate of HANA-4 is very sensitive to the microstructure determined by the final annealing temperature. Therefore, it is suggested that the final annealing at 470°C is more desirable for improving the corrosion resistance of HANA-4 alloys at least in the corrosion environments tested in this study.

3.3 Oxide Microstructure

Fig. 5 shows the oxide microstructure in the oxide/metal interface region of HANA-4 annealed at 470°C after 1000 days in the PWR-simulating loop conditions. It was revealed that the oxide microstructure consisted mainly of columnar grains in the interface region. The size of columnar grains ranged from 20 to 50 nm in width and from 200 to 300 nm in length in the oxide of HANA-4 annealed at 470°C.

In the case of the final annealing at 570°C, the oxide microstructure was composed of columnar grains. However, the columnar grain size was decreased to 20 to 40 nm in width and 200 to 250 nm in length as shown in Fig. 6. As mentioned earlier, the corrosion rate of HANA-

Table 2. Characteristics of the Precipitates Observed in HANA-4

Final annealing temperature	Precipitate type	Frequency	Crystal structure	Chemical composition (at.%)	Average particle size
470°C	ß-enriched $Zr(Nb,Fe,Cr)_2$	Major Minor	BCC HCP	69.34Zr-30.66Nb 54.12Zr-31.85Nb-9.15Fe-4.87Cr	70nm
570°C	ß-enriched $Zr(Nb,Fe,Cr)_2$	Major Minor	BCC HCP	69.57Zr-30.43Nb 46.24Zr-37.66Nb-10.69Fe-5.40Cr	90nm

4 was increased with an increase of the final annealing temperature, which is likely to be correlated well with a reduction in size of the columnar grains in the oxide/metal interface region. It is well known that columnar grains are more desirable to reduce the diffusion rate of oxygen ions when compared to equiaxed grains since the main diffusion path of oxygen ions is a grain boundary of an oxide. Such a beneficial effect would be enhanced if the grain size of the columnar grain is increased. Therefore, it is considered that the lower corrosion rate observed in the HANA-4 alloys annealed at 470°C is attributed to the larger columnar oxide grains.

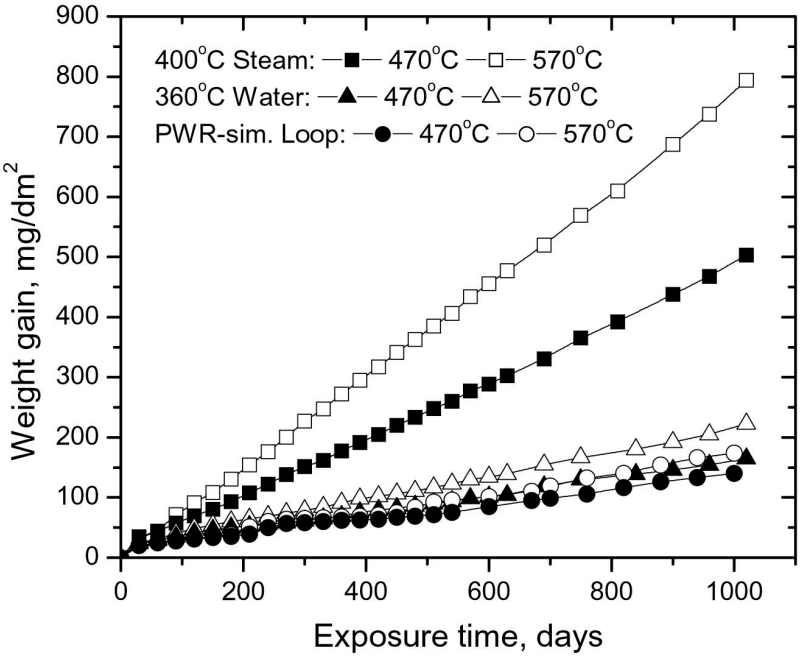

Fig. 4. Corrosion Behavior of HANA-4 Alloys which were Final Annealed at 470°C and 570°C in 360°C PWR-Simulating Loop, 360°C Pure Water and 400°C Steam Conditions

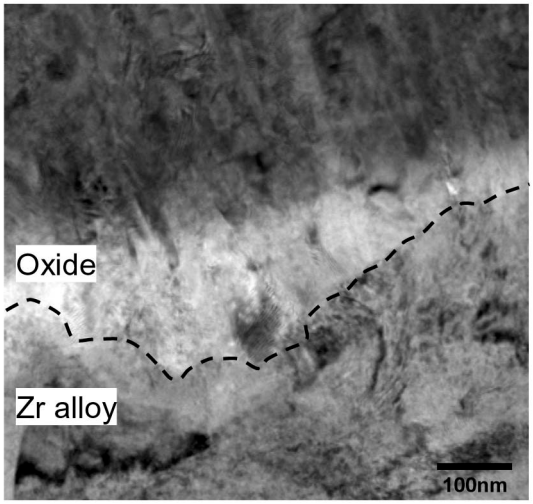

Fig. 5. Microstructure of the Oxide/Metal Interface Region of HANA-4 Alloys which was Final-Annealed at 470°C after 1000 Days in the PWR-Simulating Loop Condition

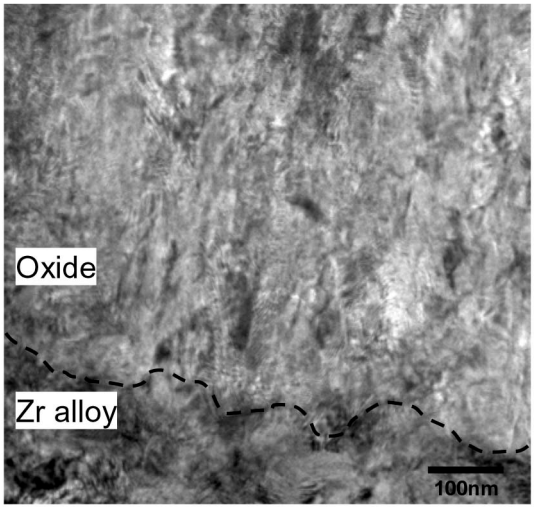

Fig. 6. Microstructure of the Oxide/Metal Interface Region of HANA-4 Alloys which was Final-Annealed at 570°C after 1000 Days in the PWR-Simulating Loop Condition

On the other hand, it is also noteworthy that the corrosion rate showed periodic behavior with exposure time in both the PWR-simulating loop and 360°C pure water conditions, as shown in Fig. 4. However, such a cyclic behavior was not observed in the corrosion kinetics of HANA-4 in 400°C steam.

In the authors' previous result[4], it was reported that the cyclic behavior observed in the corrosion of Zr alloys was closely related to the change of the oxide microstructure. Transmitted light optical microscopy revealed that the oxide consisted of multiple layers after corrosion test in the PWR-simulating loop condition[4]. It implies that the microstructure of the oxide was changed periodically during the process of oxide growth[4,5]. An oxide transition is usually accompanied by oxide cracking[6] since the internal stress accumulated during oxide growth has to be relaxed.

The characteristics of the oxide layer structure were different depending on the corrosion rate of the Zr alloy. The oxide formed with a lower corrosion rate was revealed to have a smaller total oxide thickness for the same duration, a higher periodic transition layer thickness and a larger columnar grain size, which are considered as the main features of a protective oxide for reducing corrosion rate. The HANA-4 alloys annealed at a higher temperature have a thicker oxide with more layers when compared to the alloys annealed at a lower temperature[4]. However, the thickness of the transition layer was found to be almost similar in the HANA-4 alloys even though the final annealing was changed. The main difference in the oxide microstructure with the change of the final annealing temperature is likely to be the size of the columnar grains, which was increased with the decrease of the final annealing temperature as shown in Figs. 5 and 6.

From the current investigation, it was revealed that the thickness of each single layer in the oxide with multiple layers was controlled primarily by the alloy composition regardless of the alloy microstructure. The most influential parameter that controls the oxide growth rate before the transition is considered to be the columnar grain size since the diffusion of the oxygen ions occurred at the oxide grain boundaries. The growth rate of each layer was found to be higher in the alloy annealed at 570°C. It implies that the oxide can grow faster into the Zr alloys with the fully-recrystallized microstructure when compared with the partially-recrystallized one. It is suggested that the growth rate of each layer was considerably affected by the alloy microstructure determined by the final annealing temperature.

It was shown in this study that the oxide grain morphology in the oxide/metal interface region was influenced by the alloy microstructure which was controlled by a final annealing temperature. The oxide was found to have larger columnar grains in the interface region when the alloy had a partially-recrystallized microstructure rather than a fully-recrystallized one.

From the viewpoint of an internal stress accumulated during the oxide growth, it is likely that the formation of larger columnar oxide grains can be promoted more by an alloy microstructure consisting of smaller-sized grains with a number of tangled dislocations when compared to a fully-recrystallized microstructure.

In the oxide/metal interface, the compressive stress is built up in the oxide while tensile stress is induced in the Zr alloy to neutralize the internal stress during the oxide growth. However, the stress state in the interface would be different depending on the microstructure of the Zr alloys. In the partially-recrystallized structure, the induced tensile stress could be accommodated by the dislocations in the alloy, which might induce the lower compressive stress in the adjacent oxide. When the internal stress is lower in an interface, the increase of the strain energy which is induced by the transformation from metal to oxide would be lower and the oxide would be able to become larger[7].

However, the degree of recrystallization of an alloy is not thought to be the only reason controlling the columnar grain size. The change of the grain size and the precipitate characteristics with a final annealing temperature are also considered to play an important role in controlling oxide grain size[7].

4. CONCLUSION

The microstructure, the corrosion behavior and the oxide properties were examined for Zr-1.5Nb-0.4Sn-0.2Fe-0.1Cr (HANA-4) alloys which were subjected to a final annealing at 470°C and 570°C. HANA-4 was found to have ß-enriched phase with a bcc crystal structure and $Zr(Nb,Fe,Cr)_2$ with a hcp crystal structure with ß-enriched phase being more frequently observed compared with $Zr(Nb,Fe,Cr)_2$. The corrosion rate of HANA-4 was increased with an increase of the final annealing temperature in the PWR-simulating loop, 360°C pure water and 400°C steam conditions, which was correlated well with a reduction in size of the columnar grains in the oxide/metal interface region. The oxide growth rate of HANA-4 was considerably affected by the alloy microstructure determined by the final annealing temperature.

ACKNOWLEDGMENTS

This study was supported by KOSEF and MEST, Korean government, through its National Nuclear Technology Program.

REFERENCES

[1] Y. H. Jeong, S. Y. Park, M. H. Lee, B. K. Choi, J. H. Baek, J. Y. Park, J. H. Kim and H. G. Kim, *J. Nucl. Sci. Tech*., **43**, 977 (2006).
[2] G. P. Sabol, J. ASTM Int., 2, Paper ID JAI12942 (2005).
[3] P. Bossis, D. Pecheur, K. Hanifi, J. Thomazet and M. Blat,

J. ASTM Int., **3**, Paper ID JAI12404 (2006).
[4] J. Y. Park, S. J. Yoo, B. K. Choi and Y. H. Jeong, *J. Alloy & Com*., **437**, 274 (2007).
[5] A. Yilmazbayhan, E. Breval, A. T. Motta and R. J. Comstock, *J. Nucl. Mater*., **349**, 265 (2006).
[6] A. T. Motta, A. Yilmazbayhan, R. J. Comstock, J. Partezana, G. P. Sabol, B. Lai and Z. Cai, *J. ASTM Int*., **2**, Paper ID JAI12375 (2005).
[7] J. Y. Park, B. K. Choi, S. Y. Yoo and Y. H. Jeong, *J. ASTM Int*., **5**, Paper ID JAI101129 (2008).